Design and Performance of a Power Train for Mild-Hybrid Motorcycle Prototype

Mattia Morandin, Marco Ferrari, and Silverio Bolognani

***Abstract*—Low weight and volume are the principal requirements for electric components in hybrid motorcycles, and the energy storage system (ESS) is the most important part that contributes to this issues. This paper deals with the choice of the best ESS and with the optimization of the hybrid power train in two-wheeled vehicles. A methodology of investigation is given in order to recognize all the data necessary to find the best technology and size for the ESS. The techniques adopted for the design of the electrical machine (EM) are also reported. Furthermore, simulations with finite elements (FE) and mathematical software, in order to predict the EM and the drive performances, are presented. Efficiency maps from FE simulations are also given. Different kind of ESSs are compared with the goal to choose the best solution balancing cost, volume and weight for a reference motorcycle. The whole power train has been practically realized and the new hybrid vehicle has been tested first in appositely test bench and also in a small private racetrack. The measured experimental results are presented.**

***Index Terms*—Hybrid electric vehicle, SPM machine, electric drive, mild-hybrid motorcycle.**

I. Introduction

In recent years, interest for mild hybrid electric vehicle (HEV) is growing up, mainly for fuel saving and emission reduction, [1], [2]. In the motorcycles the transition from conventional Internal Combustion Engine (ICE) vehicles to HEVs is very attractive but there are still open issues and possible optimizations to be investigated in order to optimize the size and the weight of the electric parts on-board. The energy storage system (ESS) in HEVs is the most critical part of the propulsion system. Its principals requirements are low weight, volume, cost, but conversely it is required high power (performance), high energy density (range), lifetime, and reliability. The different type of energy sources complement drawbacks of each single device, [3]. Typically the ESS is composed by different kind of technologies i.e., Ultracapacitor, [4], LiPo, [5], NiMH, [6], and lead-acid [7]. The power provided by the ESS is a function of the power demand and braking regeneration power imposed by the vehicle during driving cycles [8]. In this work a simple but effective solution of motorcycle hybridization has been designed in order to improve the performance of the original vehicle when the torque of the ICE is low, i.e. at low rotating speeds. In order to study the performance of the vehicle a careful simulated analysis through implementation of whole model of the vehicle has been made. The chosen solution has been validated with the realization of a motorcycle prototype which has been tested on test bench and on racetrack.

This work was financed by Veneto Region by MO.Bi. project and the company leader was Aprila s.p.a..

The authors are with Department of Industrial Engineering, University of Padova, via Gradenigo 6/A, 35131 Padova - Italy (e-mail: edlab@dii.unipd.it).

978-1-4673-4974-1/13/$31.00 ©2013 IEEE

II. Power-train overview

In order to reduce the volume and the weight, the power-train architecture is composed by an ICE direct connected to a surface PM (SPM) synchronous electric machine (EM), a bi-directional single-stage power converter and an ESS. The whole system is shown in Fig. 1 and it is monitored by a Vehicle Management Control Unit (VMCU). However in the literature there are a lot of different configuration of power-trains, [9].

The motorcycle that has been chosen to realize the hybrid vehicle is Aprilia RS4 125. Since the EM is direct connected to the ICE shaft the new vehicle will be hybrid with parallel philosophy. The target of hybridization is to increase the original ICE torque at low speed, as it is reported in Fig. 2, in order to satisfy the user's requirements without increasing maximum power for complying the motorcycle standards. Fig. 2 shows by dashed-dotted line the original ICE torque, by solid line the combined one and by dashed line the EM torque. The motorcycle has been investigated by simulation approach

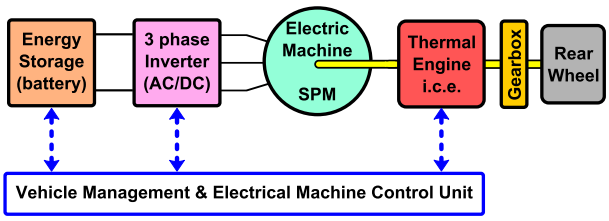

Fig. 1: Power-train sketch overview.

in order to find the most effective power train compatibly with constrains of low weight, volume and cost but with performance as higher as possible.

A. Performance of the Electrical Machine

An EM, as that considered in this work, connected to the ICE is commonly called integrated Starter-Alternator (ISA), [10]. ISA machine tasks are: ICE start-up, power boost, generating on-board of electrical energy, and regenerating braking. The original alternator has been substituted with a more powerful EM in order to satisfy the requirements in terms of torque and power as shown in Fig. 2. Since the position of the EM on the motorcycle was fixed by the old alternator, also the maximum dimensions were limited. The new EM has been designed in order to accommodate a maximum diameter of

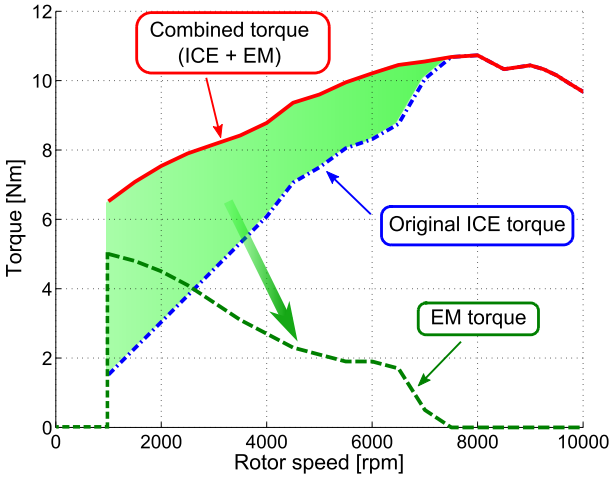

Fig. 2: ICE and combined torque

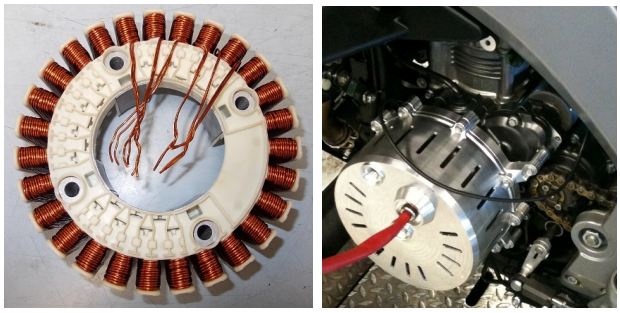

(a) (b)

Fig. 3: SPM machine prototype.

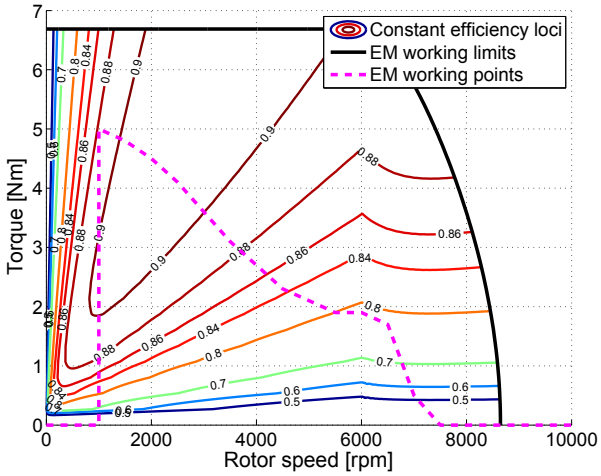

Fig. 4: SPM machine efficiency map.

135 mm and a maximum length of 62 mm. An SPM machine with outer rotor and inner stator has been developed for space saving reasons and Fig. 3 shows the prototype of the stator. A concentrated winding is also adopted in order to reduce the copper weight, cost and also Joule losses. The rated torque of the EM is 6.7 Nm, delivered up to 6000 rpm (even if it's not required), the peak torque is 10 Nm and the maximum speed is higher than 8000 rpm. Table I collects EM data including geometrical parameters (i.e. external diameter, stack length, pole and slots number) and electric parameters (i.e. rated phase current and voltage, phase resistance and inductance and so on). Machine performances have been estimated with Finite Elements (FE) analysis. Copper losses (1), iron losses (2) and mechanical losses (3) have been taken into account (into the EM working regions) calculating the efficiency map presented in Fig. 4. The real EM working points are also drawn to verify the effective efficiency achieved. The equations used for losses calculation are also reported. In particular copper losses are:

$$P_j = 3RI^2 \tag{1}$$

in which R is the winding phase resistance and I is the phase current. Iron losses are estimated by:

$$P_{iron} = P_{s,steel}\left(k_{hyst}\frac{f}{50} + k_{ec}\frac{f^2}{50^2}\right)\left(\frac{B}{1}\right)^2 \tag{2}$$

where $P_{s,steel}$ is the specific loss of the lamination steel (given at $B = 1\ T$ and $f = 50\ Hz$) and k_{hyst}, k_{ec} are two coefficients that indicate the contribution of hysteresis and eddy currents losses respectively. Finally mechanical losses are calculated as:

$$P_{mech} = kP_{out}\sqrt{n} \tag{3}$$

where k is a coefficient equal to $0.6 \div 0.8$, [11], P_{out} is the mechanical power (in kW) and n is the rotor speed expressed in rpm.

B. Performance of the electric converter

The power converter, that has been adopted for this hybrid motorcycle, is a bi-directional single-stage topology. It is a simple but effective three-phase half-bridge converter, its DC bus is direct connected to the vehicle battery pack whose voltage, V_{DC}, is fixed to 450 V. The power converter characteristics are reported in Table II and Fig. 5 shows the inverter prototype.

TABLE I: Electric machine parameters.

Parameter	Value
Pole number	18
Slot number	27
External stator diameter	156 mm
Stack length	35 mm
Type of magnet	Ferrite
Rated torque	10 Nm
Rated phase current	25 A_{pk}
Rated phase voltage	220 V_{pk}
Phase resistance	75 $m\Omega$
Phase inductance	230 μH
External Phase inductance	120 μH
Magnet flux linkage	0.024 $V_{pk}s$
Rated speed	9000 rpm
Average efficiency	90 %
Weight	5 kg

TABLE II: three-phase inverter parameters.

Parameter	Value
Number of phases	3
Type of switch	IGBT
Switching frequency	20 kHz
Dead time	2 μs
Maximum DC bus voltage	500 V
Rated AC current	25 A_{pk}
Rated AC voltage	220 V_{pk}
Average efficiency	90 %
Weight	3 kg

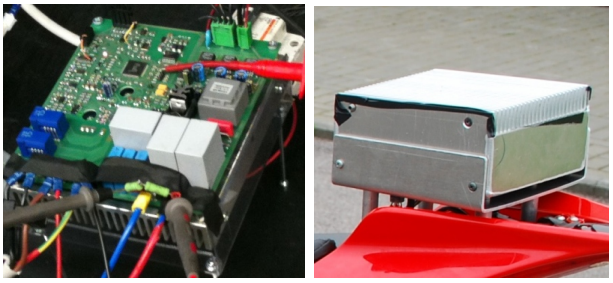

(a) (b)

Fig. 5: Three-phase inverter prototype.

In order to estimate the average inverter efficiency in the hybrid vehicle working points a losses analysis has been carried out. The dominant factor in the total power losses of power converter are the conduction losses and switching losses in the devices. The estimate efficiency in all drive working points has been computed by using the device information, that has been reported in its datasheet, [12]. The switching losses, P_{SW}, and conduction losses P_{ON} with IGBT devices have been calculated by following formulae, [13]:

$$P_{SW} = (E_{on} + E_{off})F_{SW} \quad (4)$$

$$P_{ON} = V_D I_D \quad (5)$$

where I_D and V_D is the current and the voltage of the device respectively, F_{SW} is switching frequency, E_{on} the turn-on switching energy and E_{off} turn-off switching energy. These energies are proportional to device current and for example are $E_{on} = 2\ mJ$ @ $30\ A$ and $E_{off} = 0.65\ mJ$ @ $30\ A$. (4) and (10) have been used to calculate the total losses of electrical drive and also the power consumption of the converter control can be included and it is estimated in the worst case as $10\ W$. The converter efficiency in the torque vs rotor speed plane has been reported in Fig. 6. The estimated average efficiency is more than 90 %.

C. Energy storage system (ESS)

In order to estimate the energy and the power required to the ESS, the World Motorcycle Test Cycle (WMTC) has been used, [14]. With the purpose of estimating the amount of energy necessary to complete the test cycle with the philosophy in [14], it has been used a reference ESS that

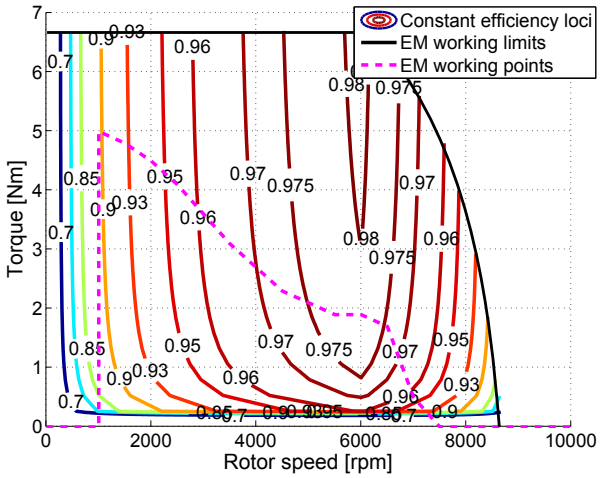

Fig. 6: Power converter efficiency map.

can be discharged/charged as the EM demands. In this way it has been developed a specific Matlab® code to analyze the telemetries and testing the strategy of use by means of an energetic approach to simulate the energy flow inside the reference ESS. Referring to Fig. 7 a graphical example of energy consumption calculation is highlighted with the red area (left side) and the analytical approach is shown by means of (6), in which the EM speed is expressed in rad/s and the EM torque is achieved by the dashed green characteristic (*EM torque*) reported in Fig. 2. The energy consumption, E_c, for

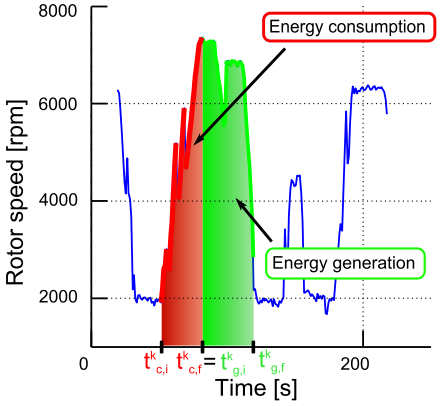

Fig. 7: Energy approach.

each interval $k-th$ is estimated in (6) and the total amount of energy in (7):

$$E_c = \int_{t_{c,i}}^{t_{c,f}} \frac{EM_{speed} \cdot EM_{torque}}{\eta_{tot}}\, dt \quad (6)$$

$$TOT\ E_c = \sum_{K_c=1}^{n_c} E_c \quad (7)$$

where t_c is the discharge interval, the subscripts $_i$ and $_f$ indicate initial and final instants of a generic interval $k-th$, n_c represents the total number of discharge interval, and η_{tot} indicates the efficiency of the whole power train.

The same approach has been used for charging intervals by means of the (8) and (9) that show the energy generation, E_g

for each interval $k-th$, and the total one respectively:

$$E_g = \int_{t_{g,i}}^{t_{g,f}} EM_{speed} \cdot EM_{torque} \cdot \eta_{tot}\, dt \quad (8)$$

$$TOT\ E_g = \sum_{k_g=1}^{n_g} E_g \quad (9)$$

Simulation results highlight that the required peak power results equal to $1800\ W$ during the boost phase and equal to$-1500\ W$ during the regenerative braking phase. The required peak energy during WMTC test cycle is $20\ Wh$.

In order to choose the best ESS for such HEV, Ragone chart has been used, [15], [16]. Fig. 8 shows an example of Ragone chart used to evaluate the energy storage performance of various technologies.

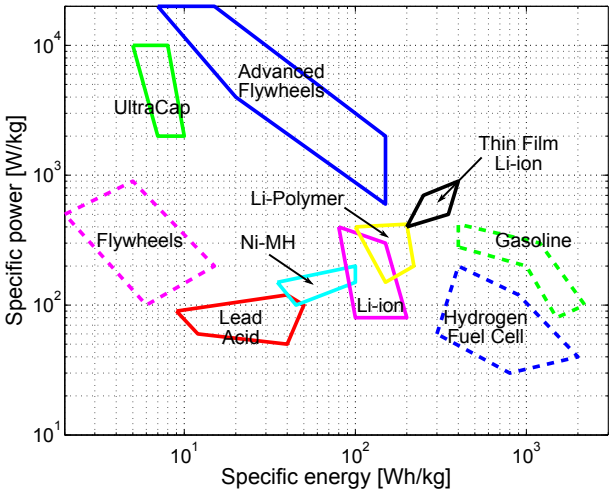

Fig. 8: Ragone chart.

From the analysis of the WMTC telemetry it is possible to achieve information of maximum power and maximum energy required by the vehicle. However a significant parameter, especially in motorcycles, is the weight.Therefore in order to choose the best technology is necessary to fix the weight limit for the ESS; in this case it has been chosen equal to $10\ kg$. As consequence the Ragone chart has been modified as shown in Fig. 9. It is worth noticing that all principle energy storage devices (batteries, ultra capacitors and flywheels) might satisfy the required target of the ESS.

Since the maximum charging power required is $1500\ W$, a proper design of the ESS has to be made in order to avoid damaging batteries (because of limitations during charge). As consequence an increase of energy has to be considered ($750\ Wh$) to satisfy the constraint above, with advantages in terms of range. As highlighted by the Figs. 10 and 11 the best technologies that allow to obtain a low weight solution without increasing too much the cost of the ESS are: Li-ion, Li-Polymer and Ni-MH batteries.

As shown in Fig. 12, Ni-MH and Li-Polymer batteries technologies have been compared with the goal to choose the best solution balancing cost, volume and weight.

For cost reasons the Nickel-metal hydrate battery has been adopted as ESS. In Table III the principal parameters of ESS

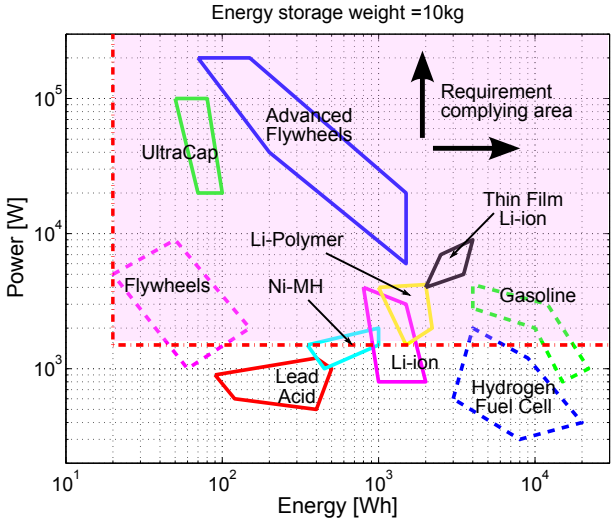

Fig. 9: Energy storage weight has been fixed at $10\ kg$.

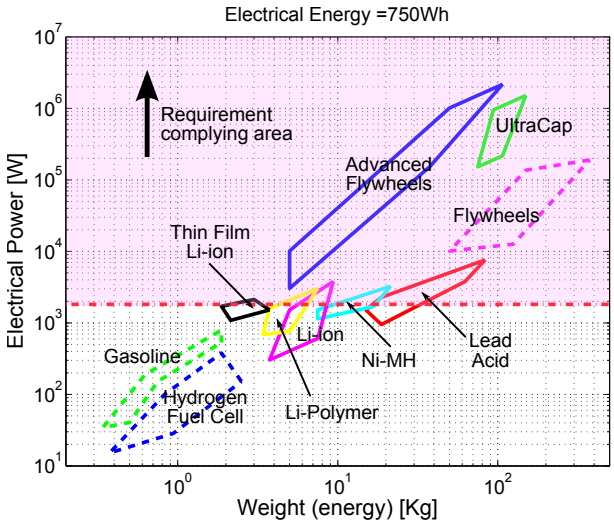

Fig. 10: Energy storage maximum energy has been fixed at $750\ Wh$ and the minimum power is $1800\ W$.

has been reported and Fig. 13 shows the adopted ESS batteries pack.

In order to investigate the efficiency of the battery pack in all working points Joule losses have been taken into account considering a simple model reported in [17]. The internal resistance of the batteries pack is $R_{int} = 2\Omega$. Such value has been shown in [18] and it allows to calculate the Joule losses in the ESS by:

$$P_{Joule} = R_{int} I_{bat}^2 \quad (10)$$

The result of this analysis is shown in Fig. 14 and the estimated average efficiency is about $96\ \%$.

III. Electric Machine Control Scheme

Referring to Fig. 15, the electric machine control scheme, implemented in VMCU, has two operating modes:

- **Motoring mode** (M): power is transferred from the ESS to the electric motor during ICE start-up or torque boost, in this phase the EM is torque controlled.

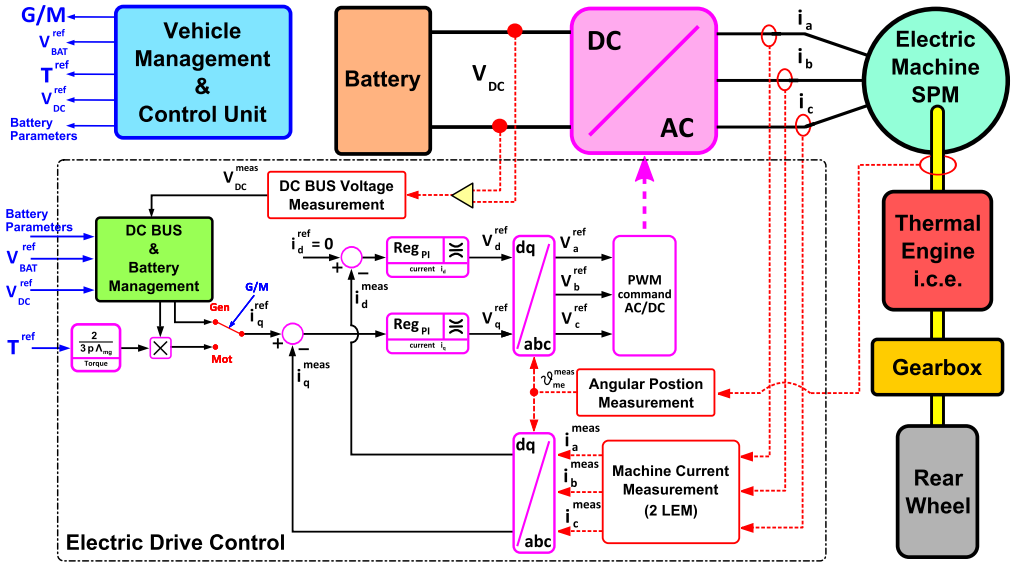

Fig. 15: HEV control scheme overview.

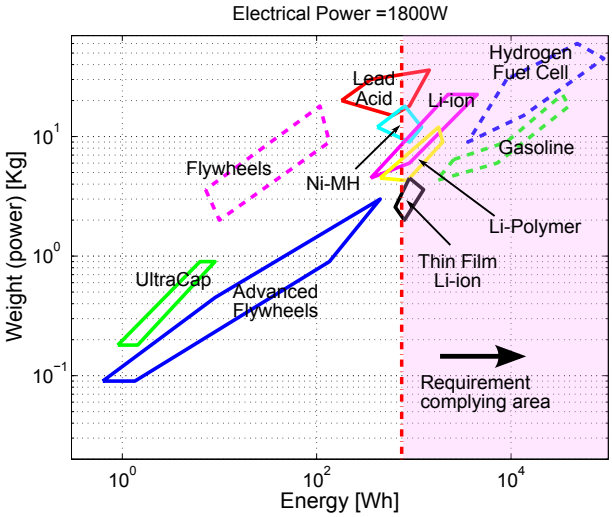

Fig. 11: Energy storage maximum power has been fixed at 1800 W and the minimum energy is 750 Wh.

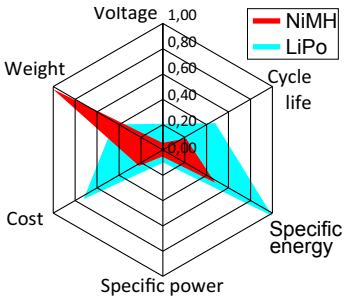

Fig. 12: Batteries comparison.

- **Generating mode** (G): the braking torque of the EM is controlled according with ESS constraints (battery current and voltage limits). Reference battery current calculation and battery voltage control are implemented inside the BMS.

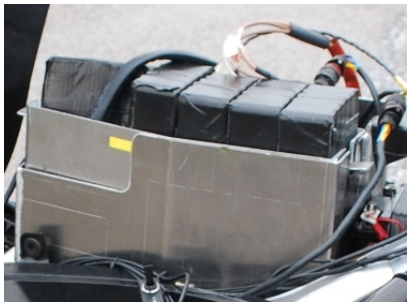

Fig. 13: Prototype Ni-MH batteries pack.

TABLE III: Battery pack parameters.

Parameter	Value
Type of battery	Ni-MH
Cell nominal voltage	1.2 V
Cell typical capacity	1.8 Ah
Cell internal impedance	75 $m\Omega$@1 kHz
Cell diameter	14 mm
Cell height	50 mm
Number of cells in series	350
Maximum battery voltage	450 V
Maximum discharge current	18 A
Maximum charge current	1.8 A
Weight	11 kg

The principle control technique adopted for both modes is therefore a torque control. In order to generate a higher level of torque the stator current vector has to be synchronized with the rotor polar axis (d-axis). To this purpose a phonic wheel composed by 46 hole detected by a magnetic pick-up has been adopted to know the rotor position. Therefore the machine is controlled to comply the MTPA (Maximum Torque Per Ampere) trajectory.
According to the MTPA control and the SPM configuration

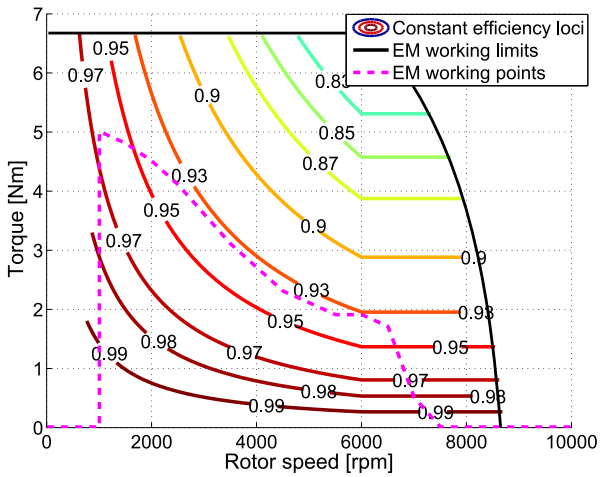

Fig. 14: Battery efficiency map.

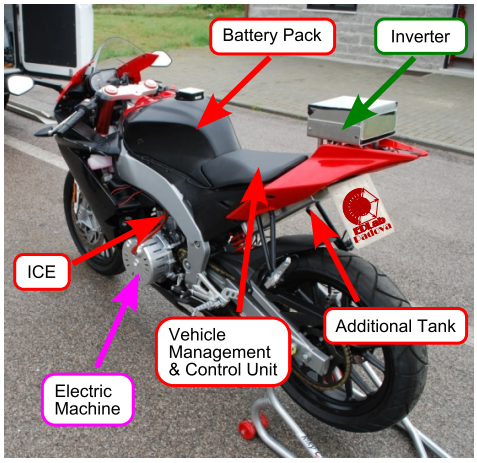

Fig. 17: Prototype HEV overview.

two current loops are implemented; the reference of first loop in the d-axis current is maintained to zero and the second one in q-axis current is related to torque demand; in this axis the reference current is positive during motor phase and negative during generating phase. Such vehicle control strategy has been implemented inside of the APX2 control unit. A VMCU prototype is shown in Fig. 16.

Fig. 16: Prototype of vehicle management control unit.

IV. Experimental prototype tests

The HEV prototype is shown in Fig. 17 and it is worth noticing that the original Aprilia RS4 125 has not been overall modified too much. The original tank has been substituted with a smaller one and placed under the motorcycle seat. In this way the space occupied by the original tank has been used for the batteries without strongly altering the vehicle. The new EM has substituted the original alternator and the EM carter support has been further increased due to the new EM larger size, whereas the inverter has been placed behind the rider above the passenger seat. The introduction of such electric components leads to an increase of weight equal to 15 kg that corresponds to 10 % of the total one.

V. Test bench measurements

Performance of the proposed HEV has been verified in appositely test bench inside the Aprilia site (Italian motorcycle company), as shown in Fig. 18. The mechanical performance of the HEV has been measured with appropriate instruments able to reconstruct the ICE shaft torque from the measured braking torque to the rear wheel. Electrical quantities have been measured by means of a Wattmeter that has been connected with the DC bus between the batteries pack and the power converter. Fig. 19 shows the performance of the electrical drive in all the working points during the motoring mode; the solid line represents the EM torque limit, the dots one show the experimental measurement points, and the dashed one reports the required EM torque according to Fig. 2.

(a) (b)

Fig. 18: Prototype HEV under test in Aprilia's test bench.

It can be noted, from the Fig. 19, that all working points that have been required during boosting phase are satisfied by the HEV power train.

VI. Race track tests

In addition the performance of the proposed HEV has been verified in a small private racetrack placed inside the headquarter of Piaggio company (owner of Aprilia), as shown in Fig. 20. Table IV reports main circuit features and weather conditions during the tests.

In order to validate the final performance of the hybrid power train compared to the conventional one, two test sessions have been made: a first session with only ICE and a second session with hybrid power train. Fig. 21 collects telemetries of two laps with electric boost (solid line) and with

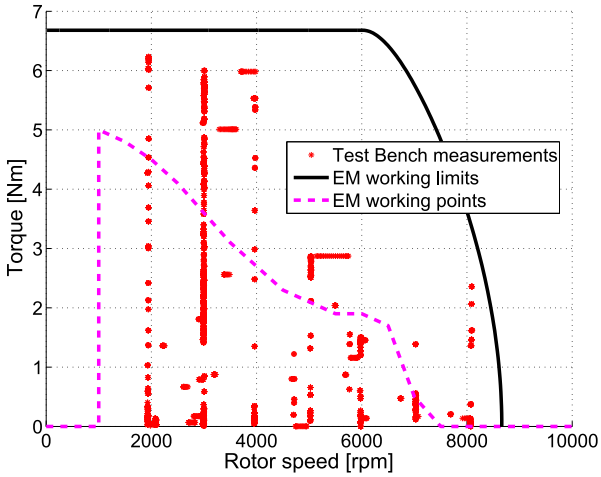

Fig. 19: Test bench performance measurements.

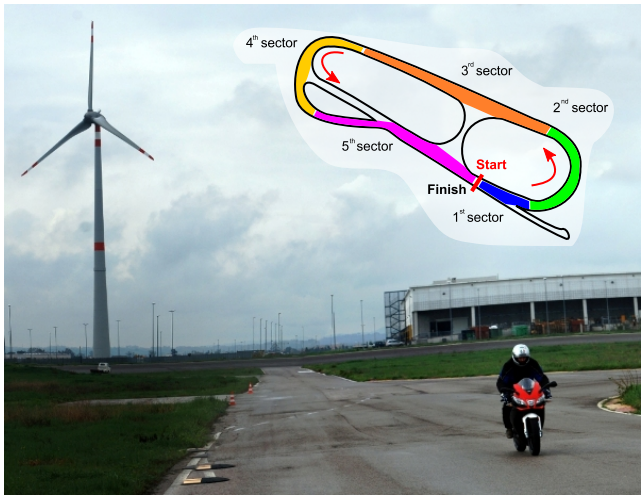

Fig. 20: Photo of prototype motorcycle during the test in Pontedera racetrack.

conventional power train (dashed line). It is worth noticing that the results confirm an increasing of the top speed (about 20%) and a decreasing of the lap time (about 10%) with the hybrid power train despite the higher weight of HEV. Furthermore, results show that the energy consumption has been compensated by the on-board energy generation, because

TABLE IV: Pontedera racetrack parameters.

Parameter	Value
1^{st} *sector* length	50 m
2^{nd} *sector* length	160 m
3^{rd} *sector* length	260 m
4^{th} *sector* length	130 m
5^{th} *sector* length	210 m
Weather condition	cloudy
Ground condition	wet
Ground temperature	15 ^oC

the amount of energy inside the ESS after two laps has not changed.

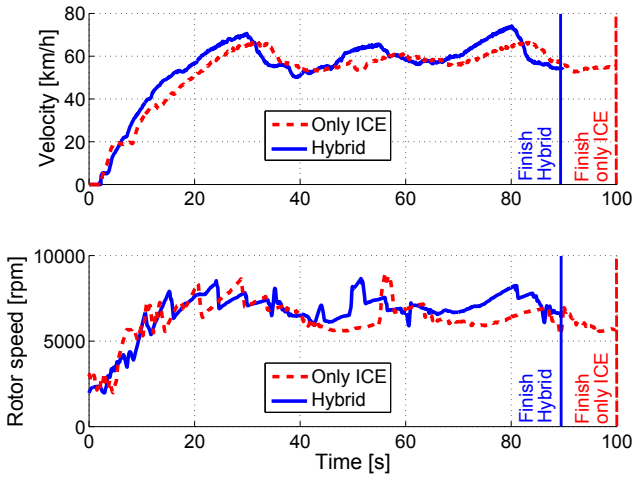

Fig. 21: Performance of two laps with and without the hybrid configuration in Pontedera racetrack.

During the test session several electrical parameters have been acquired by means of the APX2 control unit, see Fig. 22. In according with the torque strategy imposed by VMCU, the peak power during the boost phase is $1800\ W$ whereas during the regenerative braking phase is $-1500\ W$.

Figs. 23 and 24 show graphical results of acceleration and deceleration performance respectively during the four laps in Pontedera racetrack with the hybrid power train. Fig. 23 highlights that the greater contribution of the EM is given during the most important accelerations that is when the vehicle runs at low speeds and when the internal combustion engine is more lacking of torque. Fig. 24 shows that a significant part of braking energy is recovered inside the ESS.

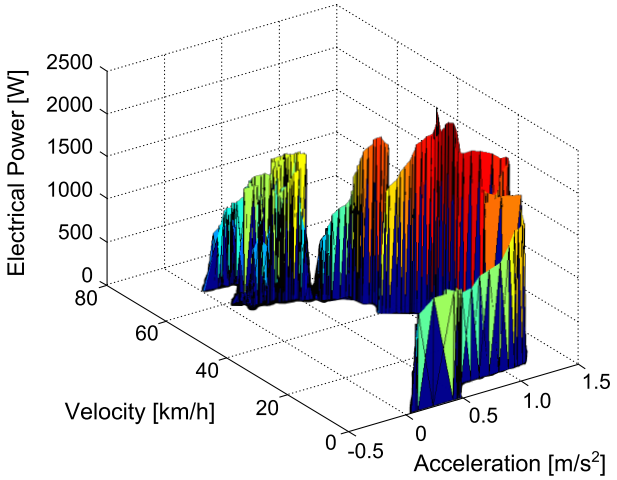

Fig. 23: Performance of acceleration in Pontedera racetrack.

VII. Conclusions

An energy conversion system suitable for hybrid electric motorcycles is proposed in this work. It is based on a SPM

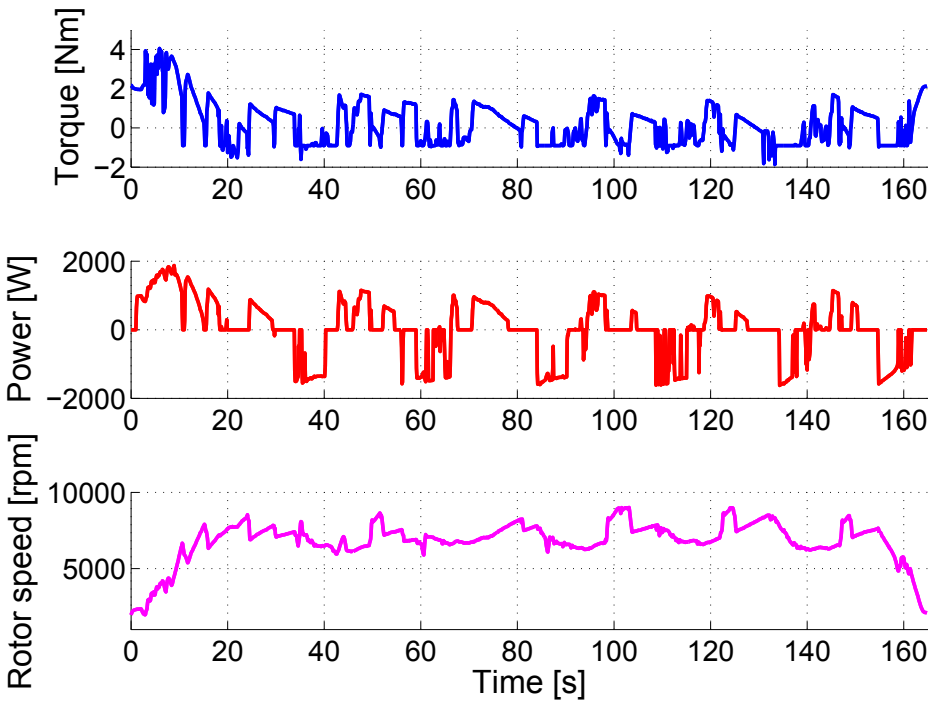

Fig. 22: Electrical characteristics of HEV have been acquired in four laps in Pontedera racetrack.

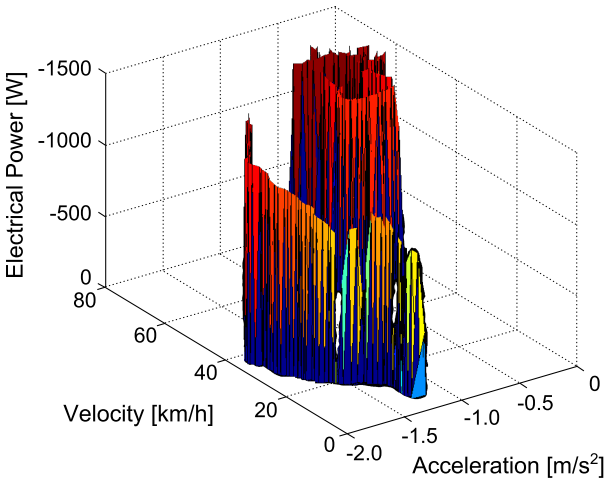

Fig. 24: Performance of deceleration in Pontedera racetrack.

synchronous machine fed by a 3-phase inverter direct connected to the Ni-MH batteries pack. The optimization and advantages of the system architecture have been analyzed through simulations and experimental tests by means of a motorcycle prototype.

VIII. Acknowledgment

Authors thank to Eng. Mosè Castiello for the precious collaboration during the realization of the experimental set-up and the execution of all tests.

References

[1] M. Ceraolo, A. Caleo, P. Capozzella, M. Marcacci, L. Carmignani, and A. Pallottini, "A parallel-hybrid drive-train for propulsion of a small scooter," *IEEE Transactions on Power Electronics*, vol. 21, no. 3, pp. 768 –778, May 2006.

[2] N. Bianchi, S. Bolognani, and M. Zigliotto, "High-performance pm synchronous motor drive for an electrical scooter," *IEEE Transactions on Industry Applications*, vol. 37, no. 5, pp. 1348 –1355, Sep./Oct. 2001.

[3] A. Khaligh and Z. Li, "Battery, ultracapacitor, fuel cell, and hybrid energy storage systems for electric, hybrid electric, fuel cell, and plug-in hybrid electric vehicles: State of the art," *IEEE Transactions on Vehicular Technology*, vol. 59, no. 6, pp. 2806 –2814, July 2010.

[4] M. Ayad, M. Becherif, S. AitCheikh, and M. Wack, "The use of supercapacitors in electrical vehicle: Modeling, sizing and control," in *Vehicle Power and Propulsion Conference, IEEE*, Sept. 2010, pp. 1 –6.

[5] T. Nobuaki, S. Imai, Y. Horii, and H. Yoshida, "Development of high-performance lithium-ion batteries for hybrid electric vehicles," *Tech. Rev., New Technol.*, 2003.

[6] D. Reisner and M. Klein, "Bipolar nickel-metal hydride battery for hybrid vehicles," *Aerospace and Electronic Systems Magazine, IEEE*, vol. 9, no. 5, pp. 24 –28, May 1994.

[7] D. Edwards and C. Kinney, "Advanced lead acid battery designs for hybrid electric vehicles," in *Applications and Advances, 2001. The Sixteenth Annual Battery Conference on*, 2001, pp. 207 –212.

[8] E. Karden, S. Ploumen, B. Fricke, T. Miller, and K. Snyder, "Energy storage devices for future hybrid electric vehicles," *J. Power Sources*, vol. 168, no. 1, pp. 2–11, May 2007.

[9] J. Cao and A. Emadi, "A new battery/ultracapacitor hybrid energy storage system for electric, hybrid, and plug-in hybrid electric vehicles," *IEEE Transactions on Power Electronics*, vol. 27, no. 1, pp. 122 –132, Jan. 2012.

[10] L. Alberti, M. Barcaro, M. Pr and, A. Faggion, L. Sgarbossa, N. Bianchi, and S. Bolognani, "Ipm machine drive design and tests for an integrated starter alternator application," *IEEE Transactions on Industry Applications*, vol. 46, no. 3, pp. 993 –1001, may-june 2010.

[11] I. Ilina, "Experimental determination of moment to inertia and mechanical losses vs. speed, in electrical machines," in *Advanced Topics in Electrical Engineering (ATEE), 2011 7th International Symposium on*, May 2011, pp. 1–4.

[12] FSBB30CH60C Smart Power Module, Fairchild Semiconductor, *www.fairchildsemi.com/pf/FS/FSBB30CH60C*, February 2008.

[13] N. Mohan, T. Undeland, and W. P. Robbins, *Power Electronics: Converters, Applications, and Design*.

[14] M. Ferrari, M. Morandin, and S. Bolognani, "Mild hybrid motorcycles: Choice of the energy storage system," in *Energy Conference and Exhibition (ENERGYCON), 2012 IEEE International*, sept. 2012, pp. 997 –1002.

[15] D. V. Ragone, in *Mid-Year Meeting of the Society of Automotive Engineers*.

[16] J. Martinez, "Modeling and characterization of energy storage devices," in *Power and Energy Society General Meeting, 2011 IEEE*, july 2011, pp. 1 –6.

[17] "Battery performance models in advisor," *Journal of Power Sources*, vol. 110, no. 2, pp. 321 – 329, 2002.

[18] KAN AA(50)1800, Kan battery co., *www.kanbattery.com*, 2004.